Ruth Román

REVIEW OF COMPUTATIONAL AND ANALYTICAL MICROMECHANICAL MODELS OF COMPOSITE MATERIALS
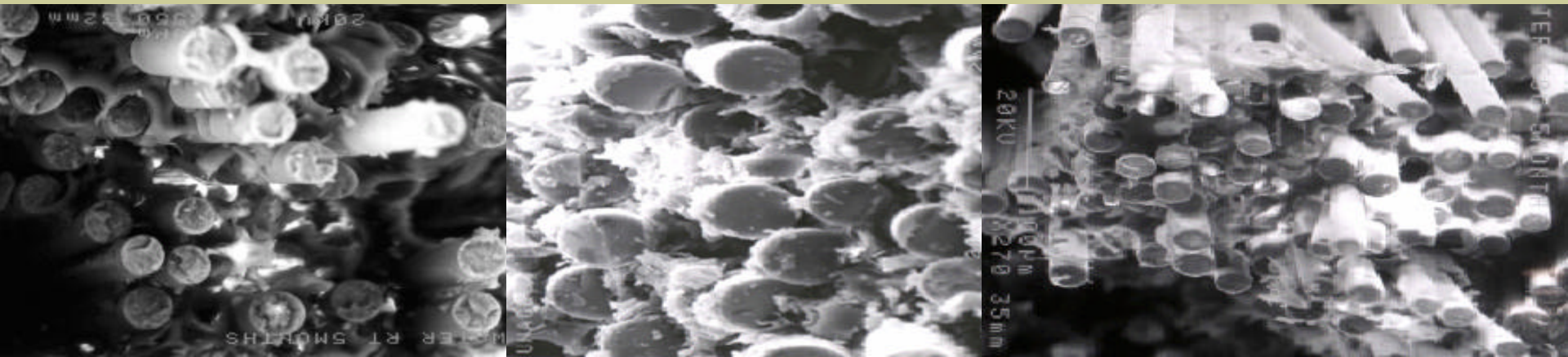
Computer modeling and FEA Simulation for Composite Single Fiber Pull-out.

Objectives:

- Explore the feasibility of applying CAD modeling and integrated CAD/FEA approach to the classical fiber pull-out problem.
- Simulate the effect of material and geometric variation on stress, stress transfer, and interface behavior, and to solve pull-out problem with irregular cross-section fibers.
- Compare results of the model prediction with the analytical solution.

Assumptions in both models:

- Isotropic linear elastic deformation behavior for both fiber and matrix.
- No sliding between fiber and matrix.
- Strains are continuous from fiber end to matrix.
- The interface is assumed to be "perfectly" bonded.

Geometrical Model:
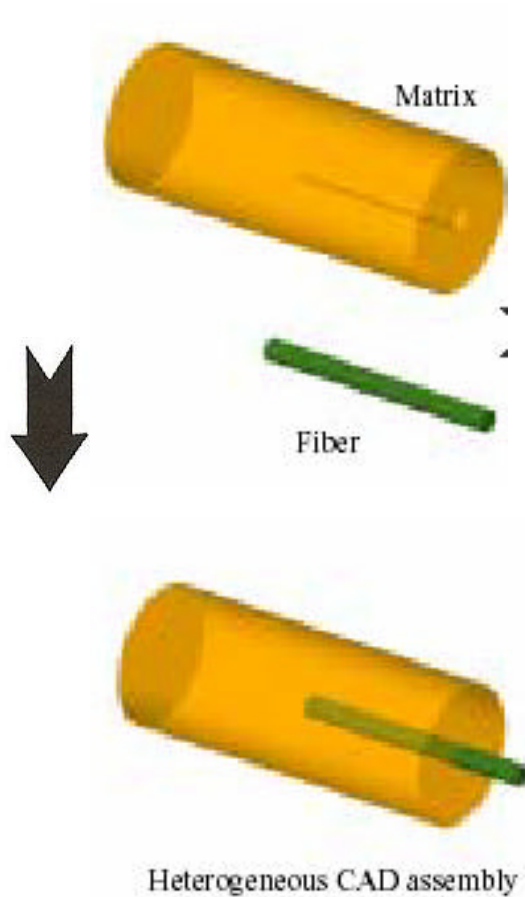
Fig. 1: Schematic of composite Fiber pull-out model.
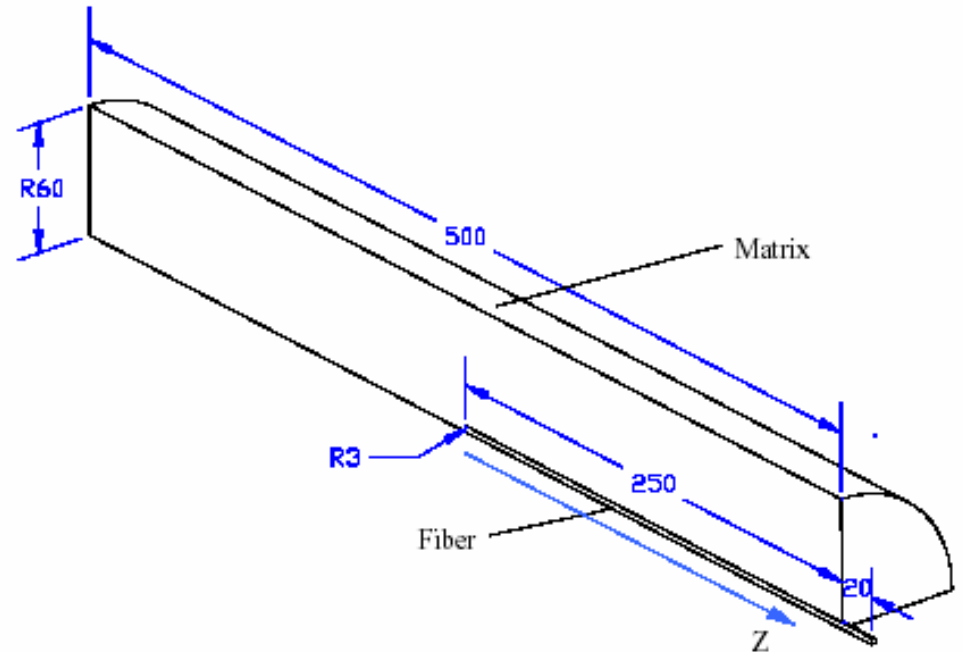
Fig. 2: Geometrical model.

Software used:
- Pro/Engineer

FEA Model:
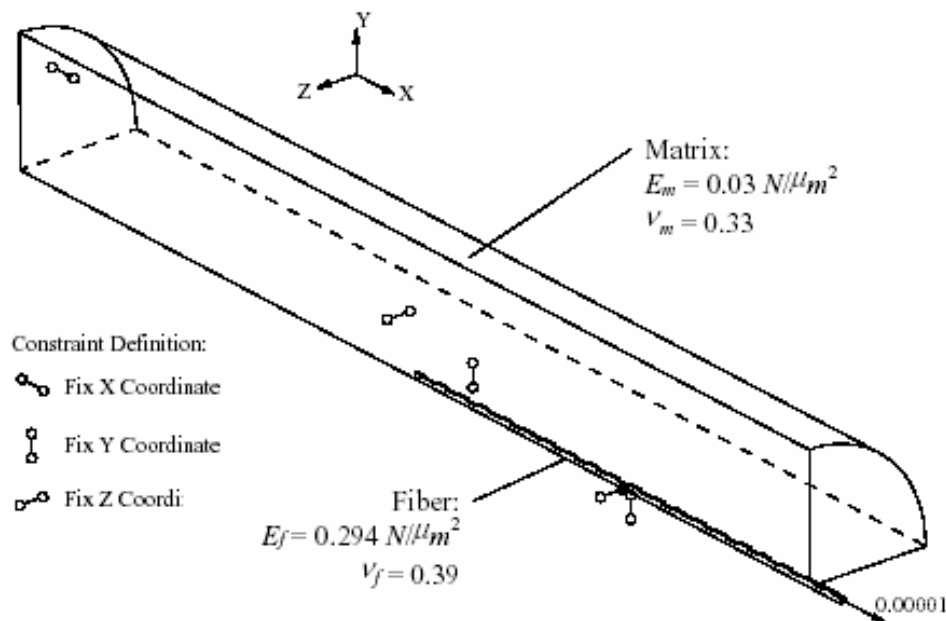
Fig. 3

- Load: 1×10^{-5} N.

- Mesh: 4867/2042/471/288 elements.

- Matrix/fiber stiffness ratios:
  Em/Ef = 1.1%, 3.4%, and 11%.

Software used:
- Pro/MECHANICA

Analytical Model:
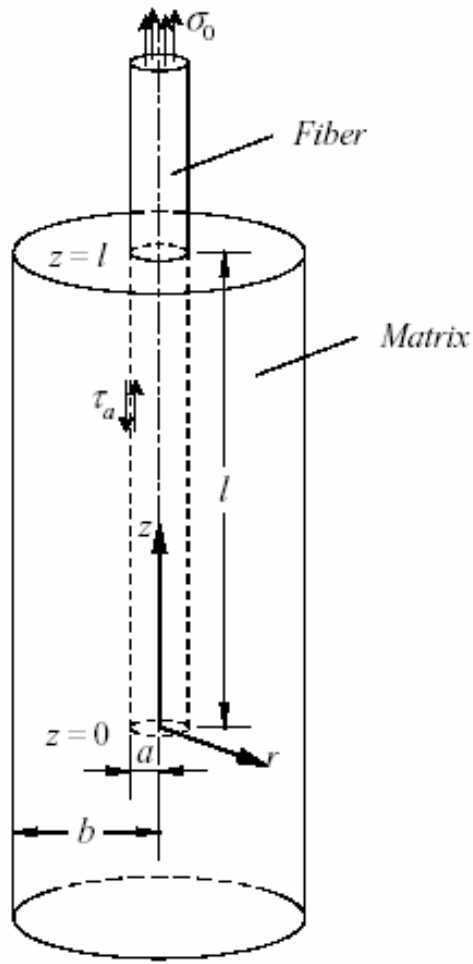
Fig. 4

$$\sigma_m = \frac{E_m}{E_f}\sigma_f + (\sigma_b - \frac{E_m}{E_f}\sigma_f)\frac{\ln(\frac{r}{a})}{\ln(\frac{b}{a})}$$

Axial stress in matrix.

$$\sigma_f = \frac{1 + \left(\frac{b^2}{a^2} - 1\right) \cdot \frac{\sinh(mz)}{\sinh(ml)} \cdot \frac{E_m}{E_f}}{1 + \left(\frac{b^2}{a^2} - 1\right) \cdot \frac{E_m}{E_f}} \cdot \sigma_0$$

Axial stress in fiber.

$$\tau_a = -\frac{a}{2} \cdot \left(\frac{b^2}{a^2} - 1\right) \cdot \frac{E_m}{E_f} \cdot \sqrt{(1+\nu_m) \cdot \left[1 + \left(\frac{b^2}{a^2} - 1\right)\frac{E_m}{E_f}\right] \cdot \left[b^2 \ln\left(\frac{b}{a}\right) - \frac{b^2 - a^2}{2}\right]} \cdot \frac{\cosh(mz)}{\sinh(ml)} \cdot \sigma_0$$

Interfacial shear stress for fiber.

Effect of embedded fiber cross section on the model prediction:

(a) Cross Shape   (b) Cross+Fillet Shape   (c) Square Shape   (d) Circle Shape
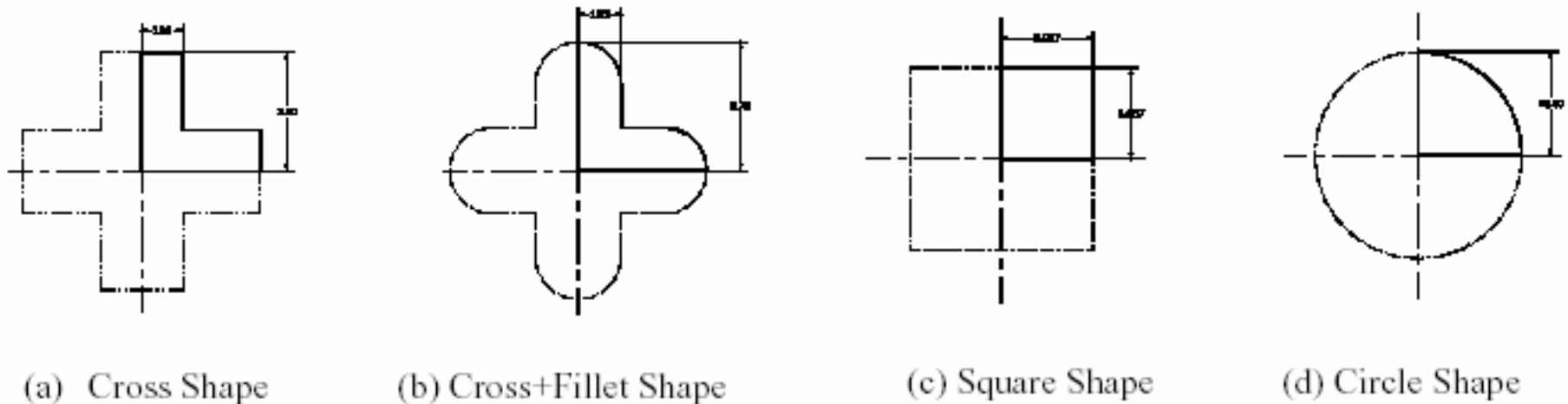
	Cross	Cross+Fillet	Square	Circle
Max Axial Stress	1.80E-06	1.77E-06	1.76E-06	1.97E-06
Max Shear Stress	3.87E-07	1.47E-07	2.36E-07	1.35E-07
Number of Element	378	671	350	471
Area of Cross Section	7.0686	7.0686	7.0686	7.0686
Length of Interface	7.0000	6.3684	5.3174	4.7124

Fig. 4. Effect of embedded fiber cross section on the interface shear stress.

Conclusions:

• Predicted stresses (fiber center axial, interface shear) are close to the analytical solution.

• Predictions are insensitive to the number of the elements used in the FEA model.

• Interface shear stress is less sensitive to the change of the matrix/fiber stiffness ratios in the range near end of the embedded fiber.

• Cross shape section fiber theoretically produced the largest interfacing shear stress, and the larger contact area between fiber and matrix.

• Circle shape section fiber produced the maximum axial stress.

Micromechanical modeling of composite with mechanical interface-Part 1: Unit cell model development and manufacturing process effects.

Objectives:

• Develop a 2D unit cell model (UCM) for MMC unidirectional laminate with the purpose to investigate both 0º and 90º oriented lamina response.

• Experimental data for comparison :

-Majumbar and Newaz (1993)

- Lerch et al. (1990)

Material:

• Matrix: Ti-15V-3Cr-3Al-3Sn (Ti-15-3)

•Ceramic Fiber: SiC (SCS6), diameter fiber: 140μm.

• Fiber volume fraction: 0.34

• Manufacturing technique: foil-fiber-foil

Software used:

• MSC/MARC2003 (commercial finite element code)

Assumptions:

• No special contact or interface elements have been used to simulate matrix-fiber bonding.

• No friction has been used.

Constituents mechanical behavior:

• Linear-elastic behavior for fiber.

• Elastic-plastic behavior for matrix.

• Isotropic behavior for both fiber and matrix.

• Plain strain.

• Standard von Mises yield criterion is assumed.

• The only damage mechanic is the fiber-matrix debonding.

Unit cell reduce scheme:
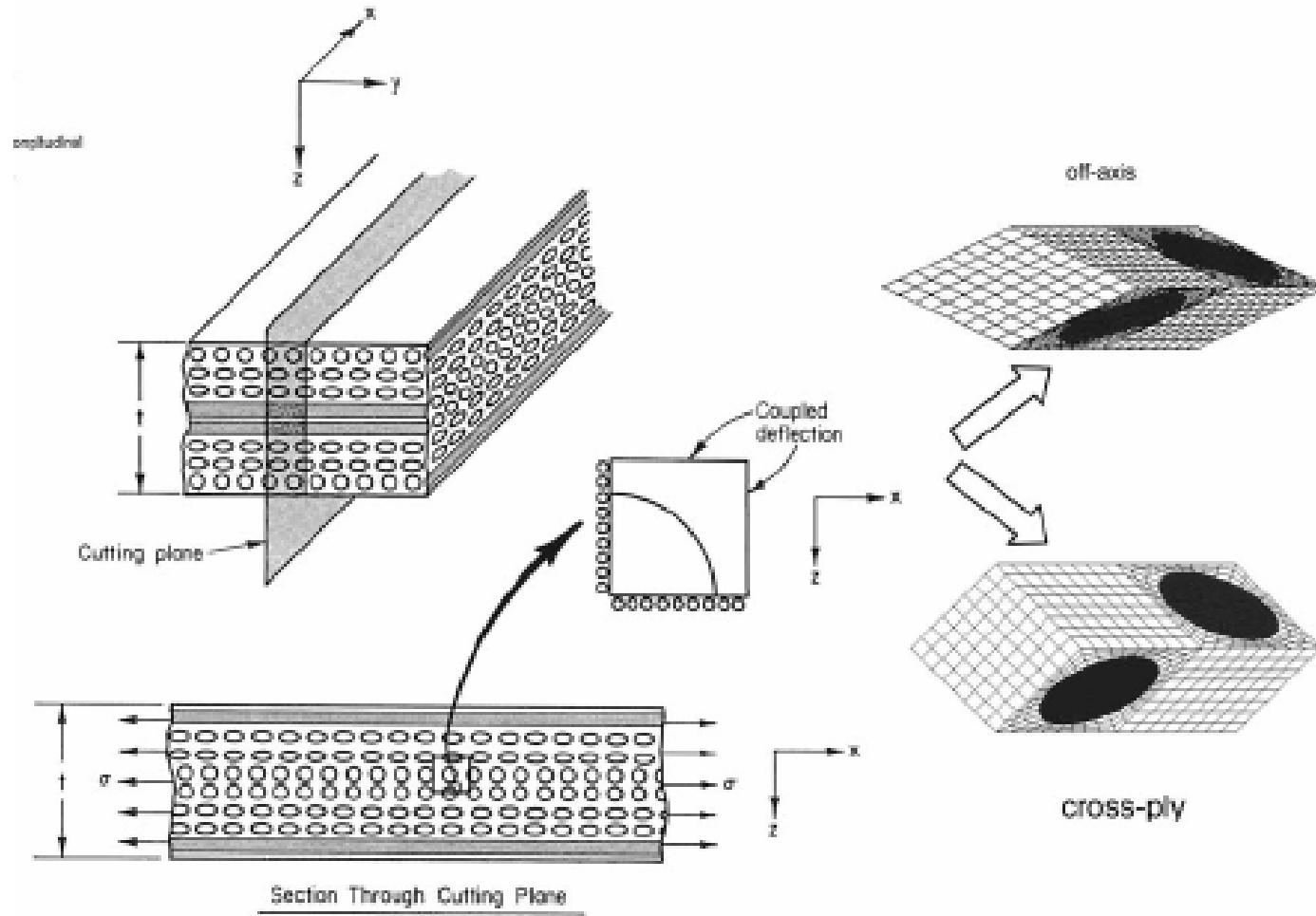
Fig. 1. Sketch of the unit cell reduction scheme. Here, the 2D UCM for the 90º unidirectional composite and the 3D UCM for a generic +?/-?, laminate is given.

FE mesh models:
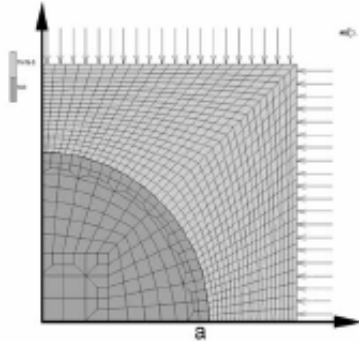
(a) FE mesh for the reference square unit cell model.
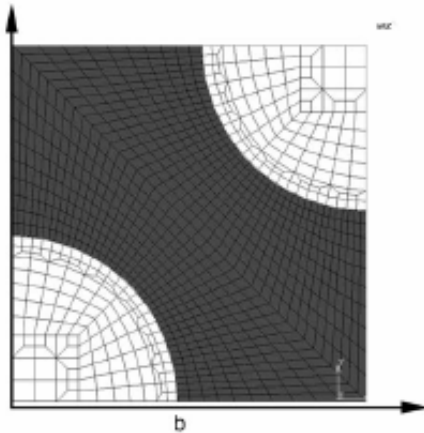
(b) Square cell from periodically square arrangement.
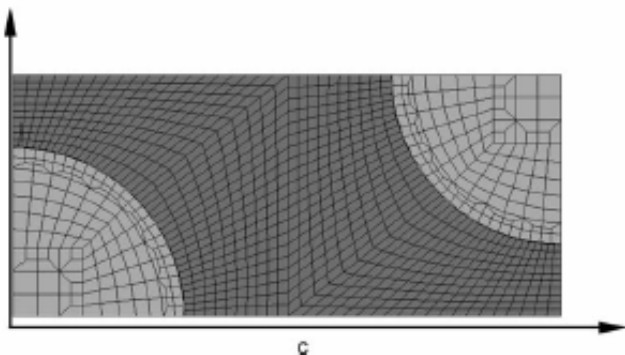
(c) Rectangular cell from periodically hexagonal structure according to microscopy results.

Fig. 2

Comparison results:
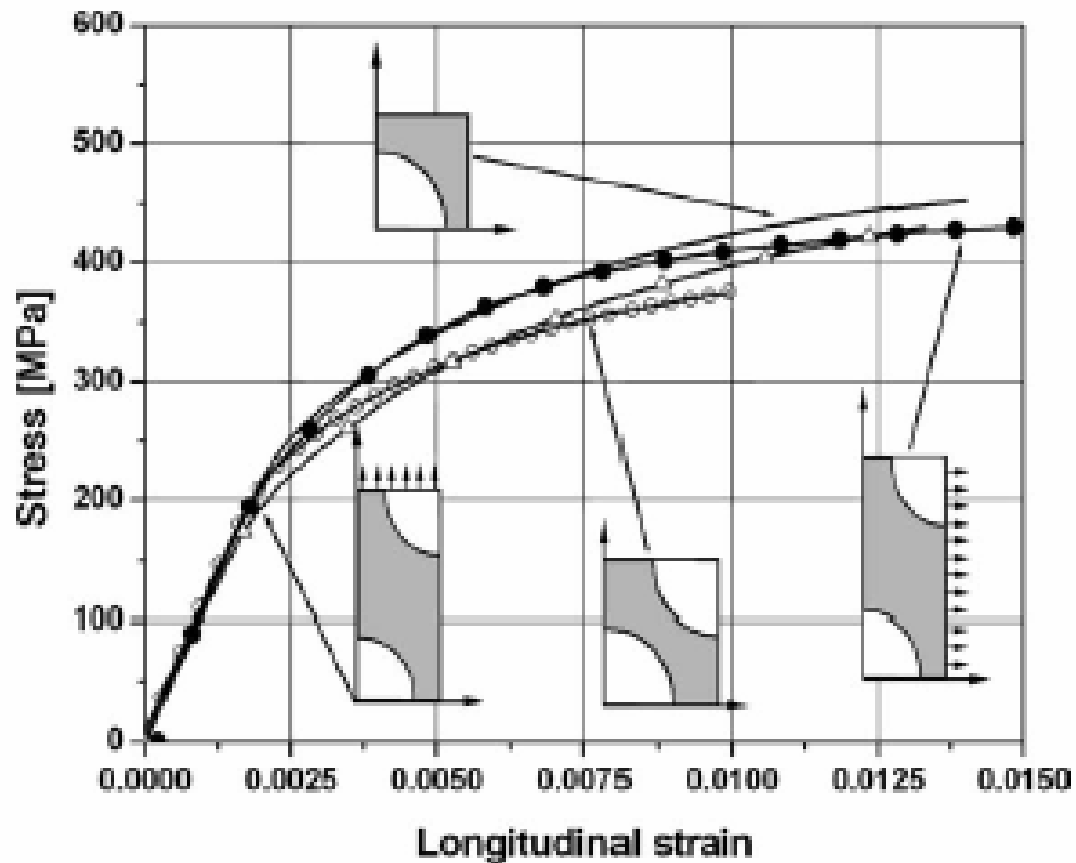
Fig. 3. Cell model effect on stress-strain response for 90⁰ laminate.

Comparison results:
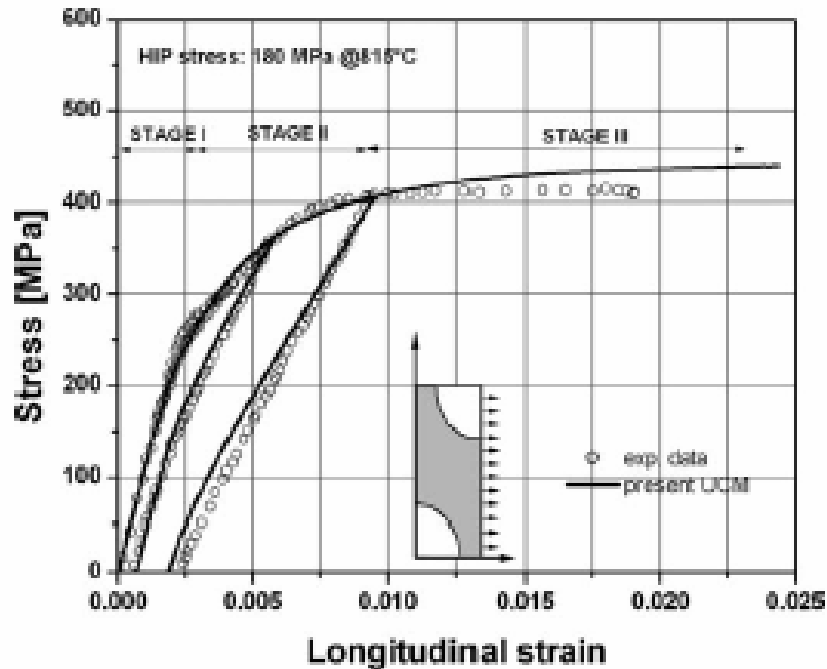
Fig. 5. Calculated stress-strain curve compared with experimental data for 90⁰ laminate (plane strain).
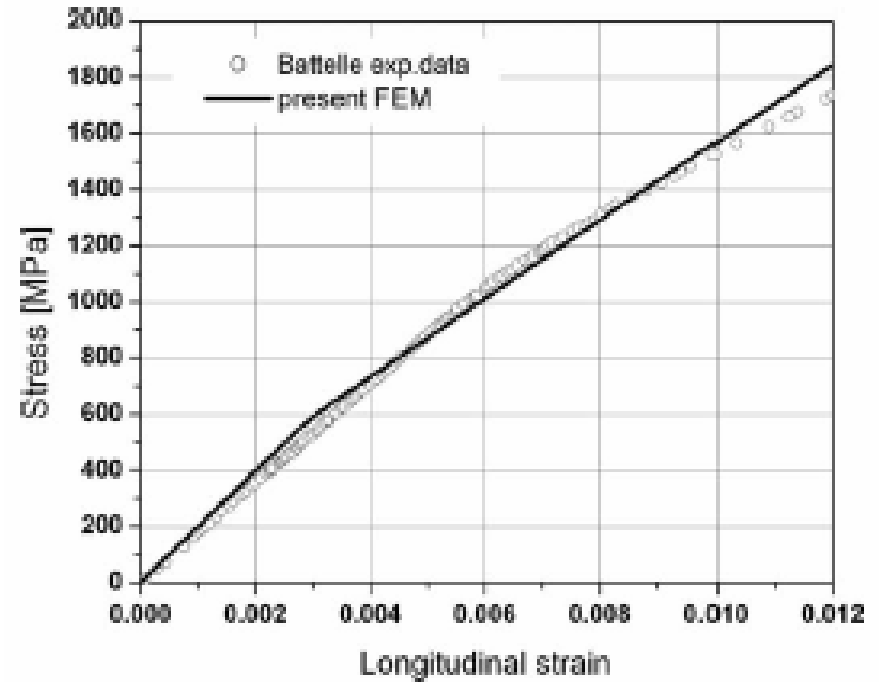
Fig. 6. Calculated stress-strain curve compared with experimental data for 0⁰ laminate (plane strain).

Comparison results:
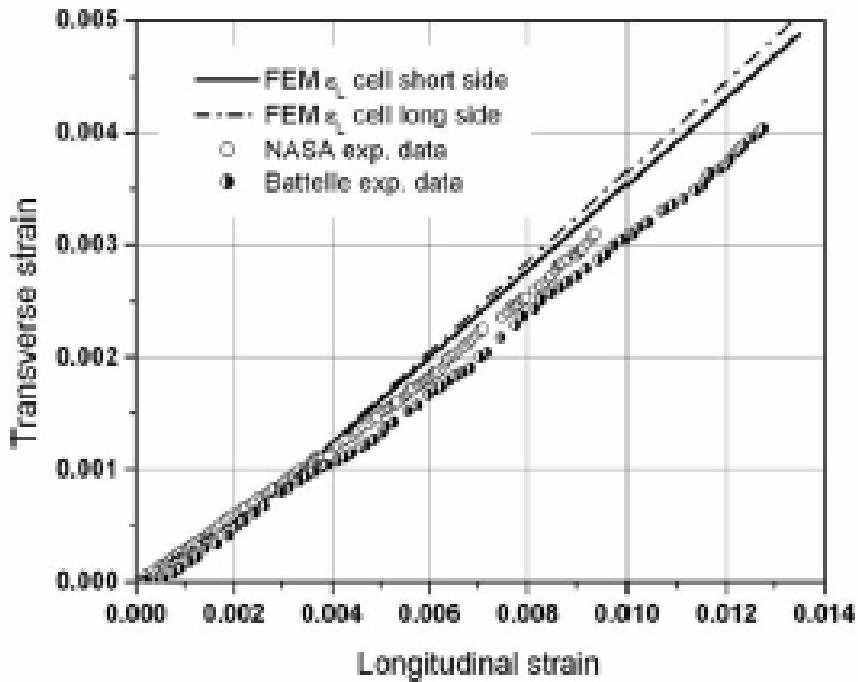
Fig. 7. Calculated transverse stress vs. strain curve compared with experimental data for 90º laminate (plane strain).
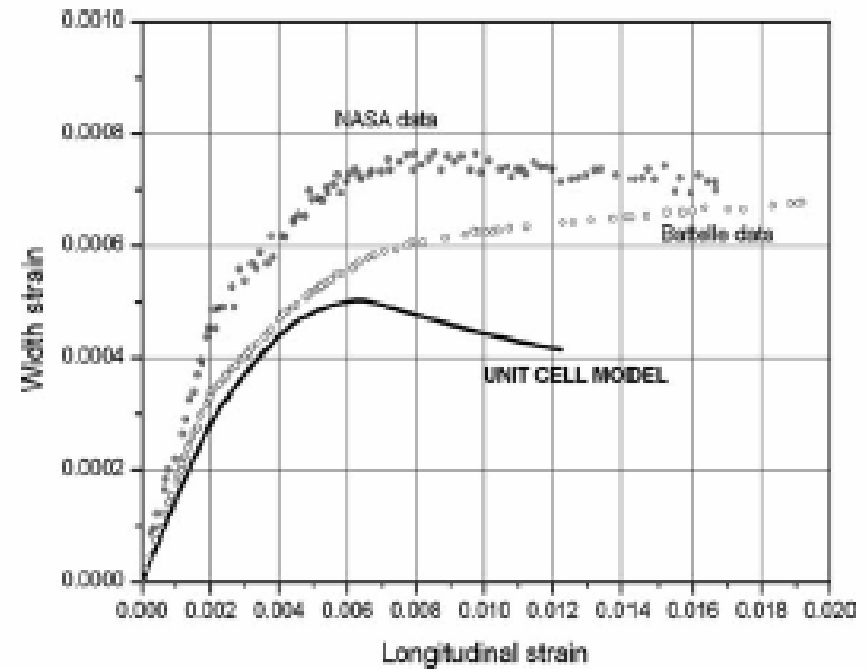
Fig. 8. Calculated transverse stress vs. strain curve compared with experimental data for 0º laminate (plane strain).

The modelling of hydrothermal aging in glass fibre reinforced epoxy composites.

Objectives:

• Effects of water absorption on glass fibre reinforced epoxy resin during immersion at different temperatures.

• Diffusion modeling.

• Comparison diffusion models with experimental results.

Material:

• Unidirectional E-glass fiber (diameter 13μm).

• Bisphenol-A epoxy resin with tertiary amine accelerator and an anhydride hardener.

• Manufacturing technique: Pultrusion.

• Fibre Volume Fraction: 48%.

Diffusion Models:

1. Fick's law and single-phase diffusion
2. Three-dimensional Fickian diffusion
3. The Langmuir model

Conclusions:

• The processes involved in absorption were found to be more complex than those of simple diffusion into the resin and are dependent greatly on the temperature.
• It is possible that the water molecules can react chemically or be trapped physically in the resin at the interface or on the fibre surface.
• The Langmuir model is more adequate than the simple Fickian model for describing the absorption process.
• The water absorption in the composite was thermally activated.
• Other possible mechanics were the reaction and combination of water molecules with the components of the composite and the progressive and irreversible damage of the material.

The role of interfacial debonding in increasing the strength and reliability of unidirectional fibrous composite.

Objectives:

• Simulate the interfacial debonding to clarify the effect of interfacial shear strength on the tensile strength and reliability of fibrous composites by using a Monte-Carlo simulation technique based on a finite-element method.

Material:

• Boron/epoxy monolayer.
• Fiber diameter : 0.142 mm.
• Fiber spacing : 0.259 mm.
• Fiber volume fraction ˜ 0.53

Models:

• FEM model.
• Shear-lag model.

FEM Model:
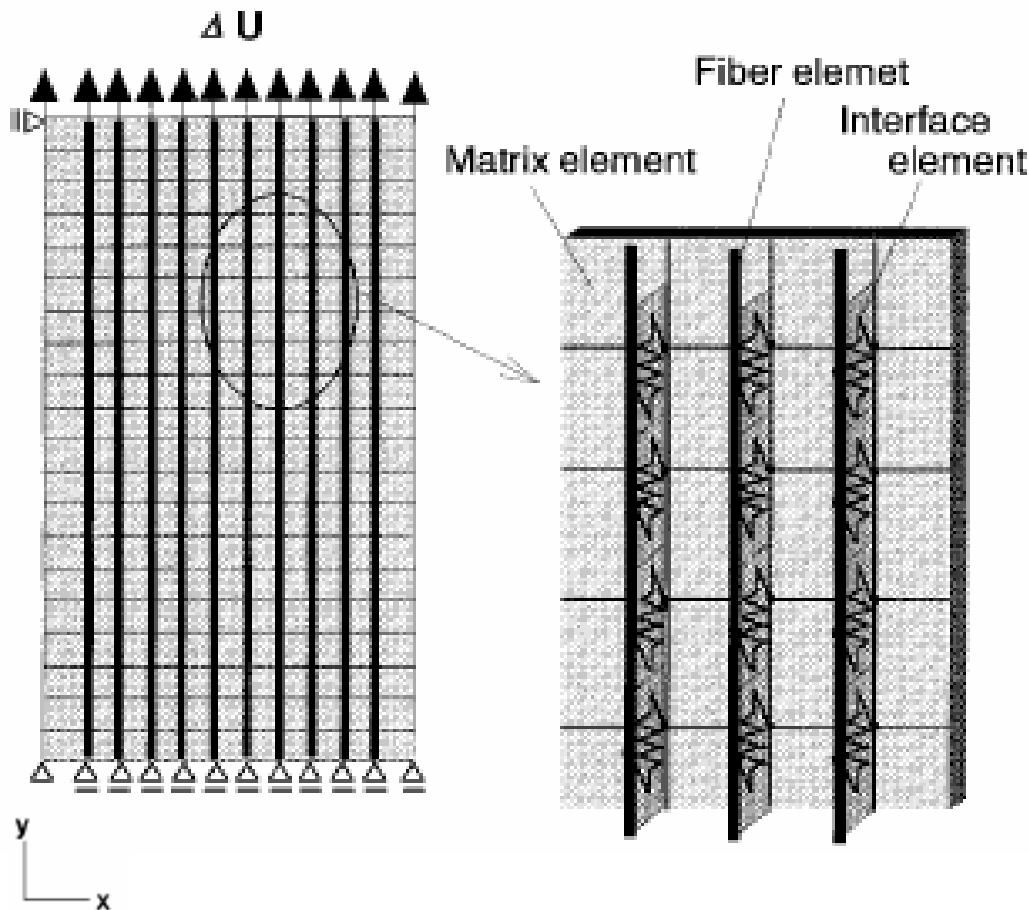
Fig. 1. Finite-element model and mesh.

Assumptions:

• Plane stress condition.

• Shear spring element representing the interfacial bond.

• Linear elastic behavior for fiber, matrix and interface.

Monte-Carlo simulation:

•500 simulations for various interfacial shear strengths; average and coefficient of variation were calculated.

Damages of matrix and interface around a broken fiber element:

(a) τᵢ = 11.7 MPa   (b) τᵢ = 20.4 MPa   (c) τᵢ = 35.0 MPa

× Fiber break

▨ Matrix cracking

Interfacial debonding
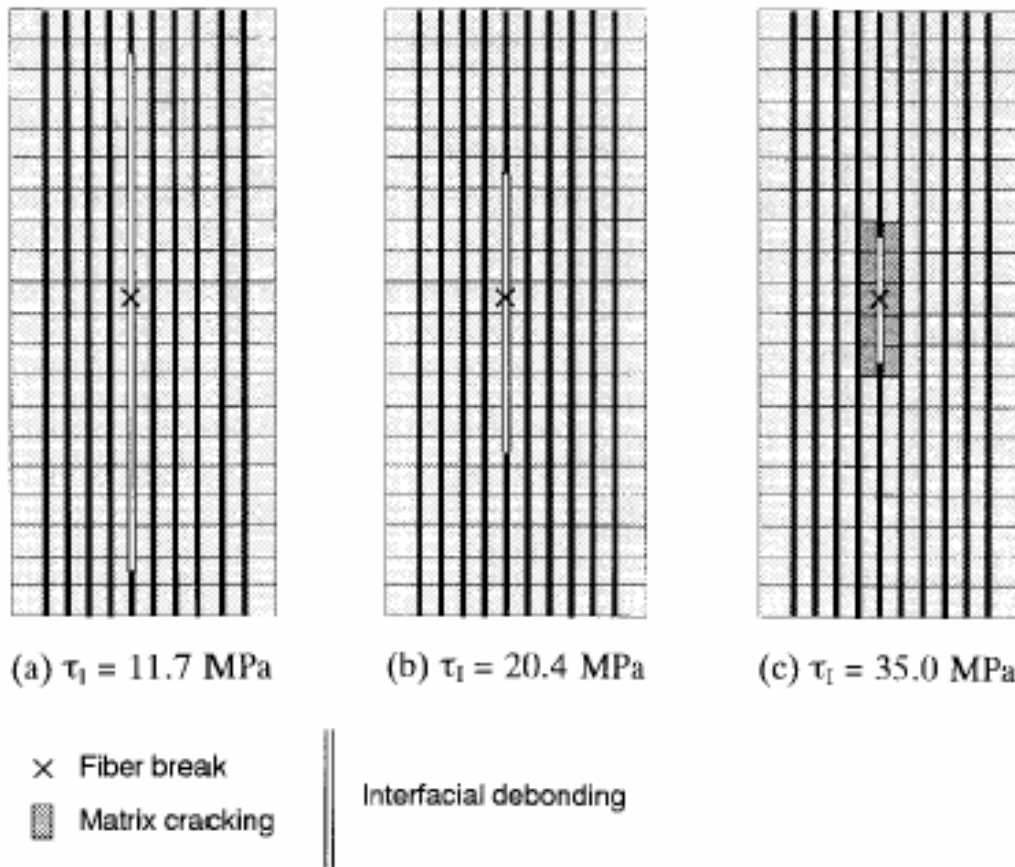
Fig. 2.

(a) t = 11.7 MPa :
- o Large-scale debonding.
- o Lowest stress concentration.
- o Poorest load-carrying capacity for the broken fiber.

(b) t = 20.4 MPa :
- o Small-scale debonding.
- o Highest load-carrying capacity.

(c) t = 35.0 MPa :
- o Largest stress concentration.
- o Matrix cracking.

Effect of interfacial shear strength on the strength and reliability:
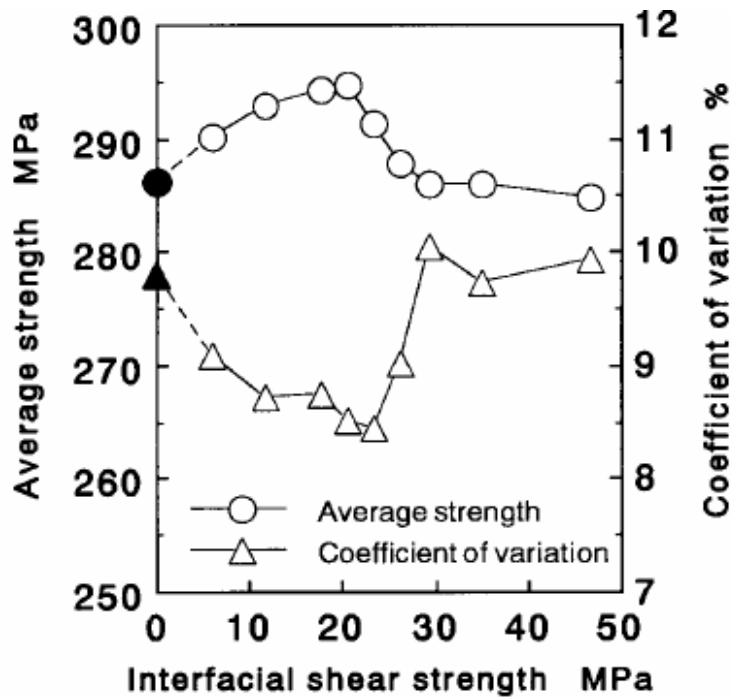
Fig. 3. Finite element model.
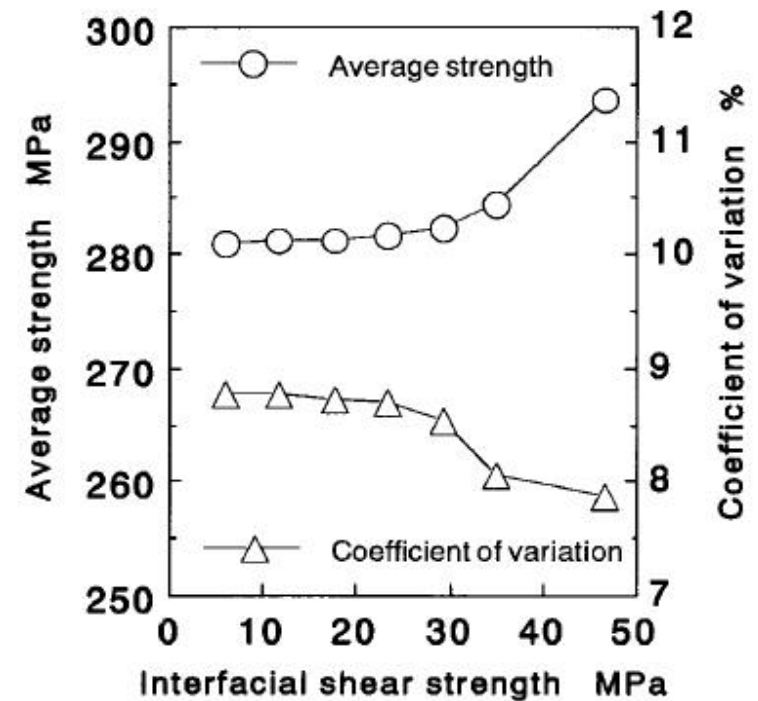
Fig. 4. Shear-lag model simulation
(Monte-Carlo simulation).

Conclusion :

• The interfacial shear strength value which increased the average strength of the composites corresponded to the value which decreased their coefficient of variation. This implied an existence of an optimum value of interfacial shear strength which can increase the strength and reliability.

• The simulated strength and reliability was closely related to the degree of damage and type following a fiber break.

• Since it was unable to simulate matrix cracking, a Monte-Carlo simulation based on a shear-lag model is unsuitable for evaluation for composites with a rigid interfacial shear bond.

An analytical-numerical framework for the study of ageing in fibre reinforced polymer composites.

Objectives:

• Develop an analytical-numerical framework for the compilation, interpretation and application of experimental data to actual engineering analysis and design taking into consideration hardening and softening ageing processes. Several examples are included to show the performance of the numerical analysis.

Experimental background review:

• Physical ageing:

- o Free volume effect.

- o Moisture absorption.

• Chemical ageing:

- o Hydrolyses.

- o Oxidation.

- o Radiation.

• Phenomenological effects.

Behaviors:

- Linear viscoelastic formulation:
    - o General relations.
    - o Kelvin model.
    - o Extension to multiaxial situations.
    - o Rheological models.
    - o Uniaxial case.
    - o Time shifting techniques.
- Non-linear viscoelastic formulation:
    - o Kelvin model.

Failure criteria:

- Failure and degradation criteria:
    - o Maximum strain criterion.

Analysis of transverse cracking and stiffness loss in cross-ply laminates with hygrothermal conditions.

Objectives:

• Examine theoretically the change in longitudinal modulus as a result of transverse ply cracking in simple cross-ply laminate taking into consideration the decrease of the mechanical properties of materials by variation of temperature and moisture.

Material:

• Simple cross-ply laminate.
• $E_0 = 41.7$ GPa
• $E_{90} = 13.0$ GPa
• $?_{12} = 0.30$
• $?_{23} = 0.43$

Geometrical model:
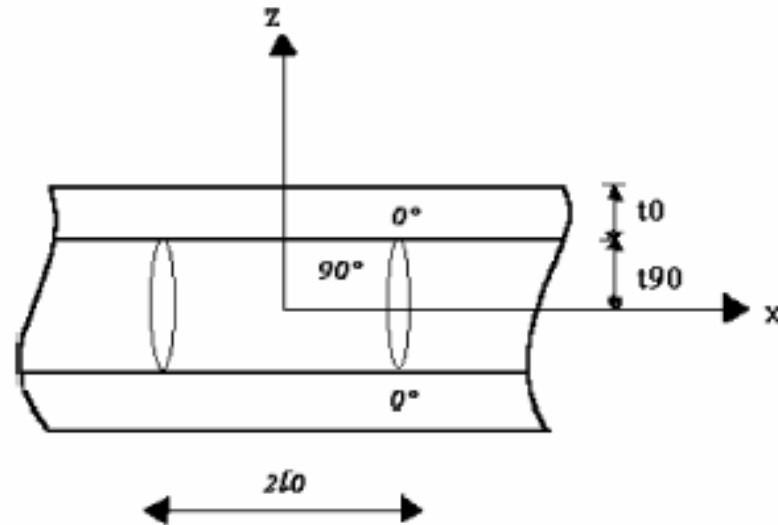
Fig. 1. Transverse cracked cross-ply laminate and geometric model.

Models:

- Shear lag model.
- Generalized Hashin's model.

Comparison with experimental data:
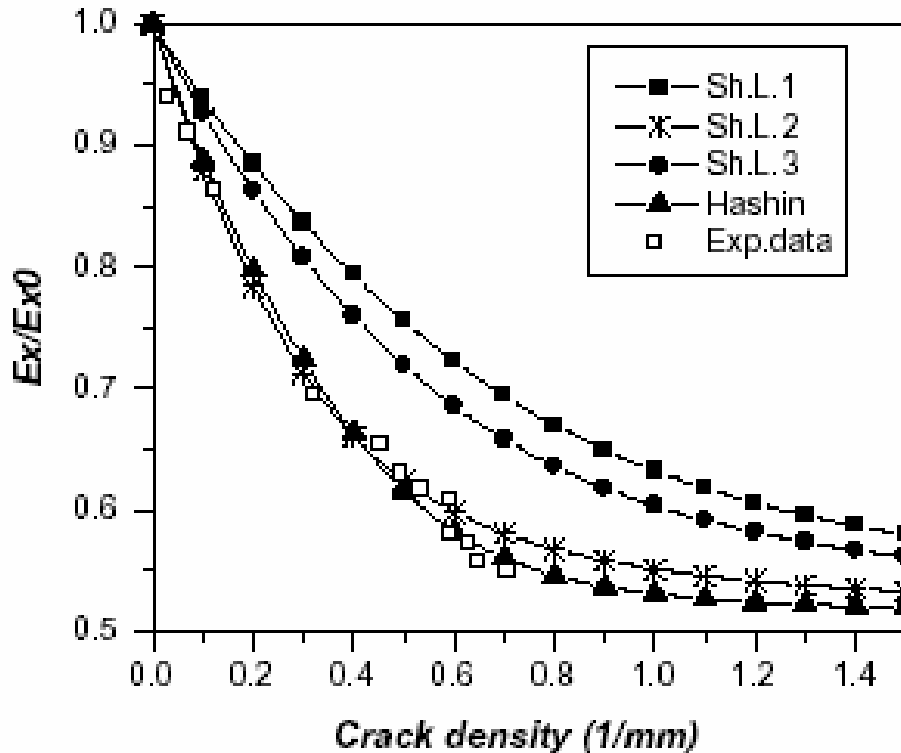
- Sh.L.1: $G=Gm/d_0$
- Sh.L.2: $G=G_{23}/t_{90}$
- Sh.L.3: $G=3\ G_{23}/t_{90}$

- Sh.L2 and Hashin's model give good prediction.

Fig. 2. Modelling predictions and experimental data for the stiffness ratio as a function of crack density. (Exp. data from Highsmith et al, 1982)

• The hygrothermal stresses and water-induced microcracks were not considered.

• Several numerical examples were presented. Graphite/epoxy composite material was selected for the examples.

Conclusion:

• Longitudinal Young's modulus is reduced with the decrease of moisture and temperature especially when the crack density becomes higher.

• Longitudinal Young's modulus is reduced with the increase of fiber volume fraction.

Modelling of stress transfer in fibre composites.

Objectives:

• Investigate the mechanics of stress transfer in simple single-fibre model composite by comparing predictive results from the finite element analysis method with experimental results gained from the technique of Raman spectroscopy.

Material:

• Kevlar 49:
  - o Linear elastic behavior.
  - o Orthotropic properties.
• Epoxy matrix:
  - o Elasto-plastic behavior.
  - o Isotropic properties.

Finite element model:

• Software: LUSAS.

• Eight-noded axisymetric element.
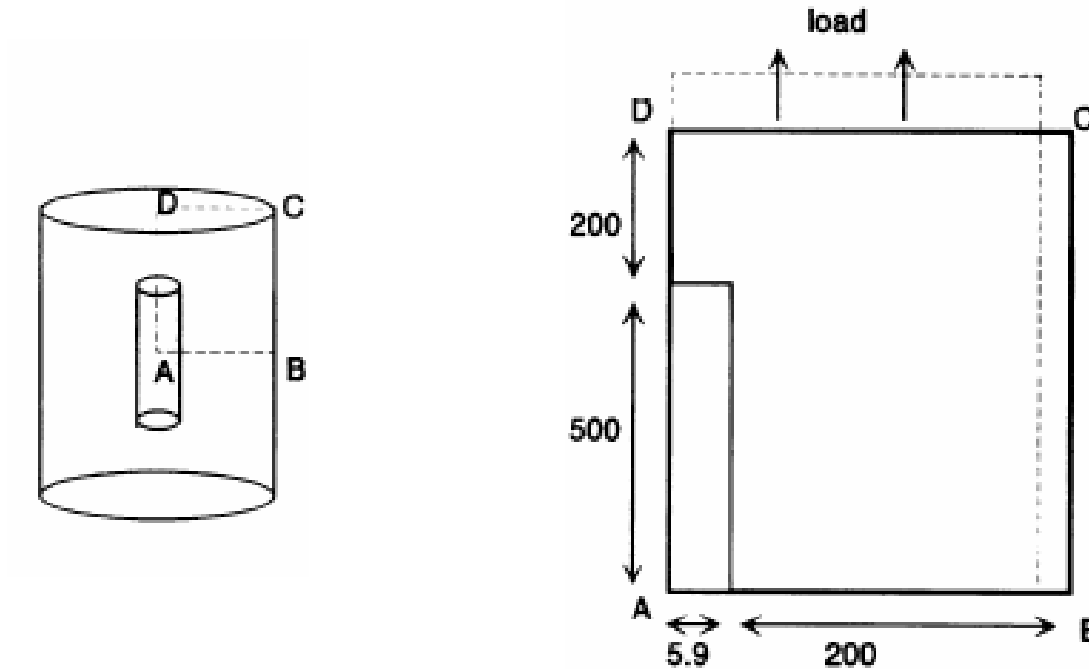
Fig. 1. The finite element model, showing the shape of the deformed grid.
Dimensions in µm.

Finite element model:

• The corner of the fibre is a singularity; stress continuity cannot be achieved.
• If the corner of the fibre is rounded and the FE grid is sufficiently fine, the singularity would not exist in the real fibre.
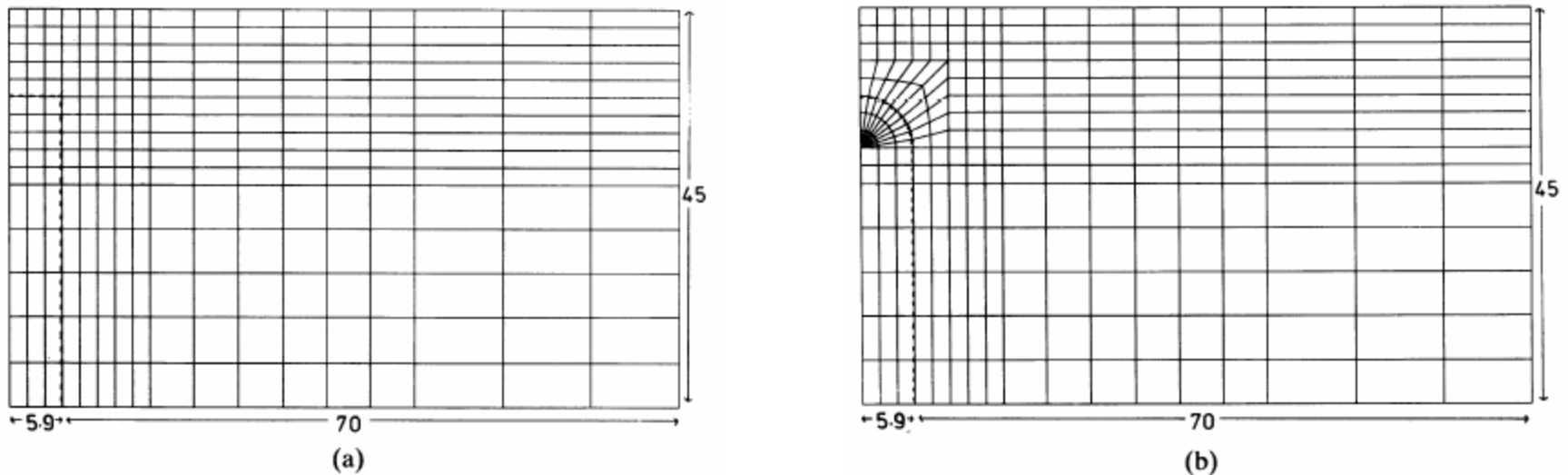
Fig. 2. The finite grids around the fibre end. (a) square end, (b) round end. Dimensions in μm.

Conclusion:

• In the FE model the stress continuity across the interface is almost perfect; this is a stringent test for the validity of the FE model.

• The behavior of the resin at the lower strain levels is mostly elastic.

• The plastic behavior of the resin has a crucial effect on the strain transfer to the fibre.

• Interfacial shear stress at the fibre end is higher for the lower strain levels and it is reduced for higher strain levels; this must arise from the necessity to balance forces around the fibre end.

• The existence of transverse compressive radial stresses arised from differences in Poisson's ratios, and are most significant at low fiber volume fractions.

Micromechanical analysis of interfacial debonding in unidirectional fiber-reinforced composites.

Objectives:

• Investigate the fiber–matrix debonding phenomena in unidirectional composites with homogeneous, isotropic and linearly elastic constituents using the finite element method.

• Evaluate the first failure loci (FFL), which provide the average strains for the initiation of fiber–matrix debonding, and the overall stiffness corresponding to several interface damage configurations.

Unit Cell (UC):
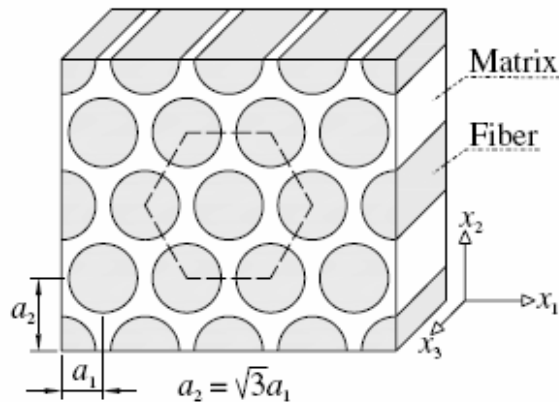
Fig. 1. The unidirectional composite with hexagonal symmetry.
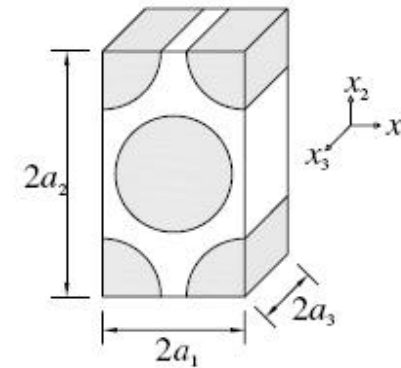
Fig. 2. The adopted 3-D UC.

Material:

- Fiber volume fraction = 0.60551
- Ef/Em = 31.304
- Poisson's ratio: Fiber   = 0.18
                      Matrix = 0.38

Finite element model:

• Software : ANSYS 6.1

•The matrix and the fibers are modeled by linearly elastic isoparametric brick elements with eight nodes and six faces.

• The interface is modeled by both contact elements and brittle-elastic joint elements.
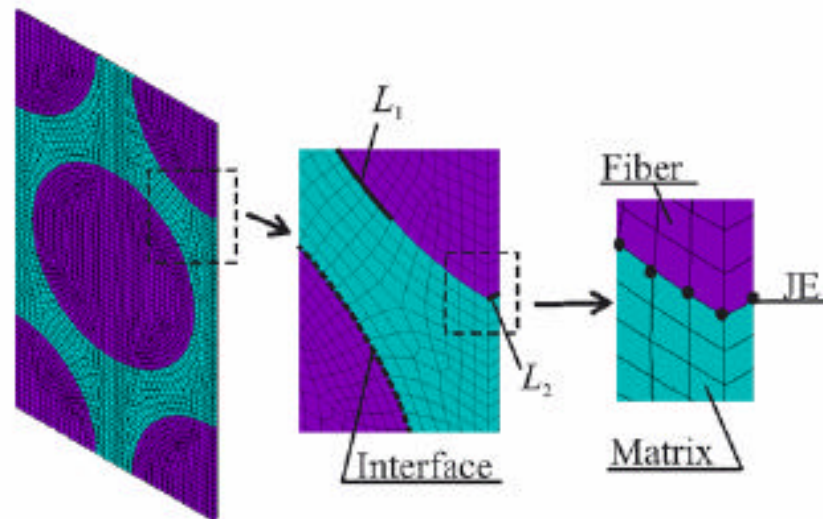
Fig. 3. The finite element mesh adopted in the computation.

Assumptions:

• The displacement field may be decomposed in a linear part and a periodic one.

• The damage is localized at the interface.

Conclusions:

• After failure, the behavior of the interface is characterized by two possible states: (I) the interface is open (the stiffness decrease is high);

    (II) the interface is closed (the stiffness decrease is low).

• The effects of the mesh dependence are not found to be significant.

• The first failure is followed by a high and abrupt decay of the overall stiffness and strength.

• The amount of debonded surface depends on the interfacial strengths.

• The instantaneous moduli depend on the configuration of the interfacial damage.

Fem mesh dependence:
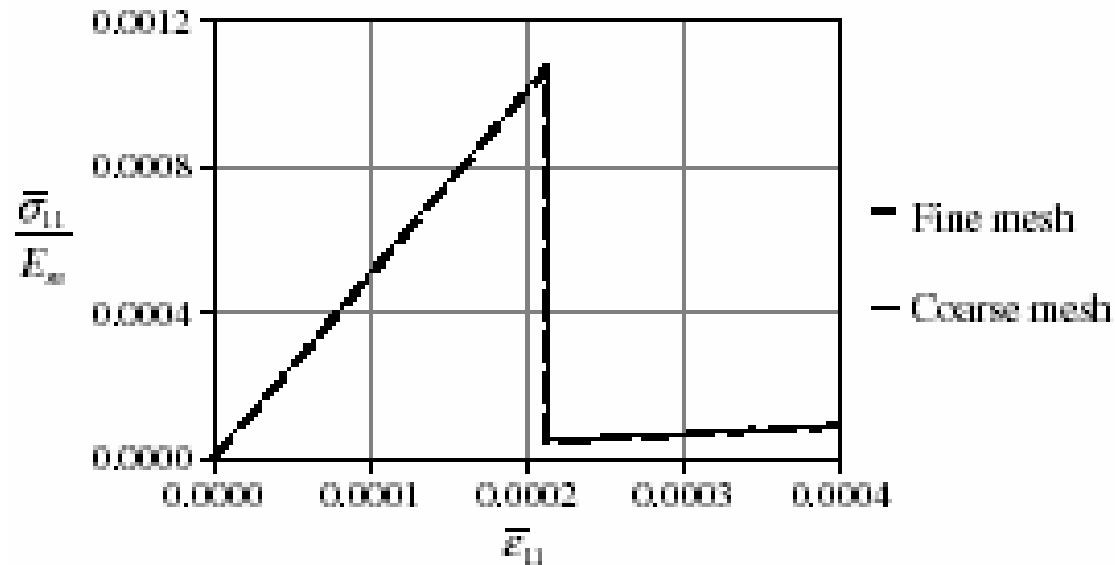
Fig. 4. The overall stress–strain relationship $s11 = Em - e11$ in the case $emn = 0$ Vmn ? 11.

Deformed mesh:
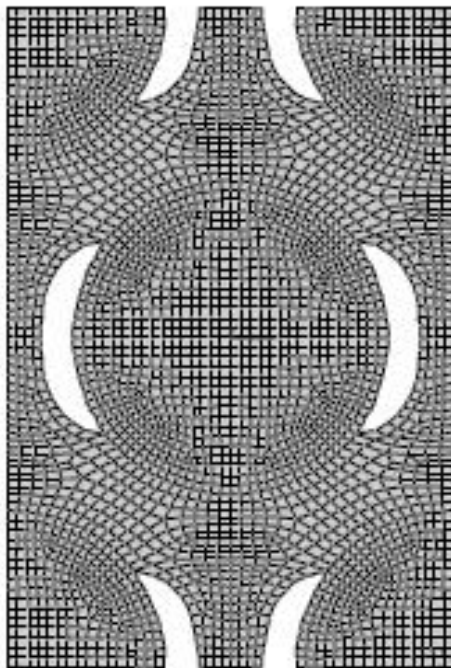
Fig. 5. Case 2.
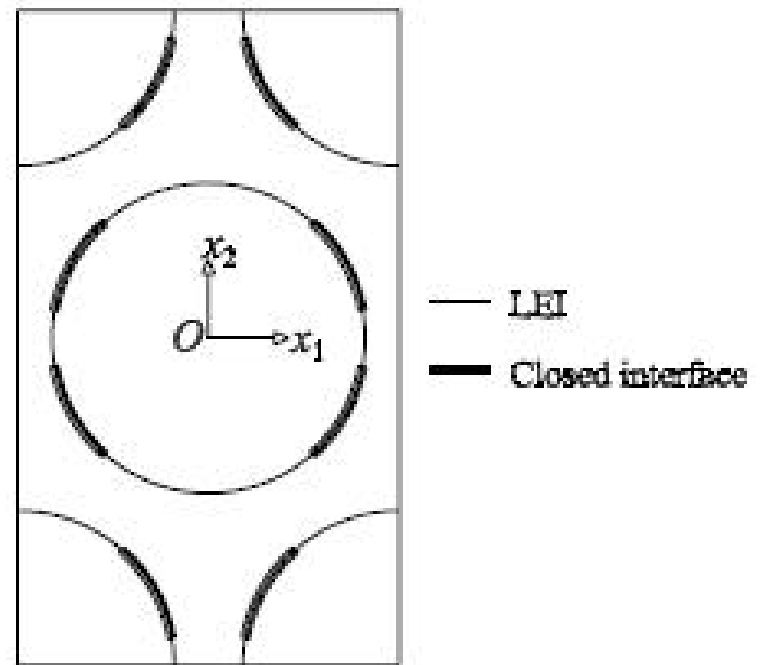
Fig. 6. Case 3.

Deformed mesh:
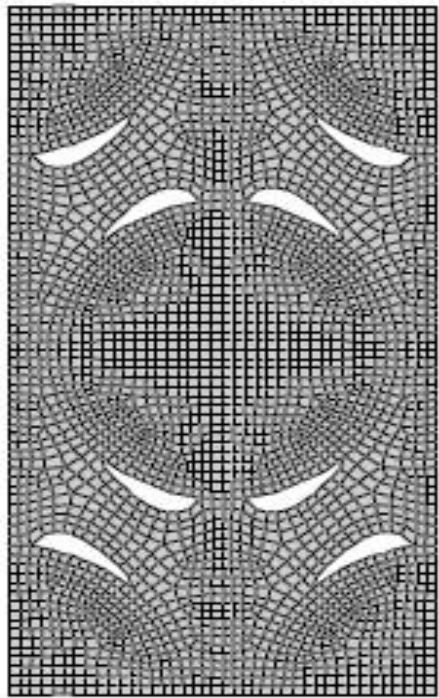
Fig. 7. Case 5.
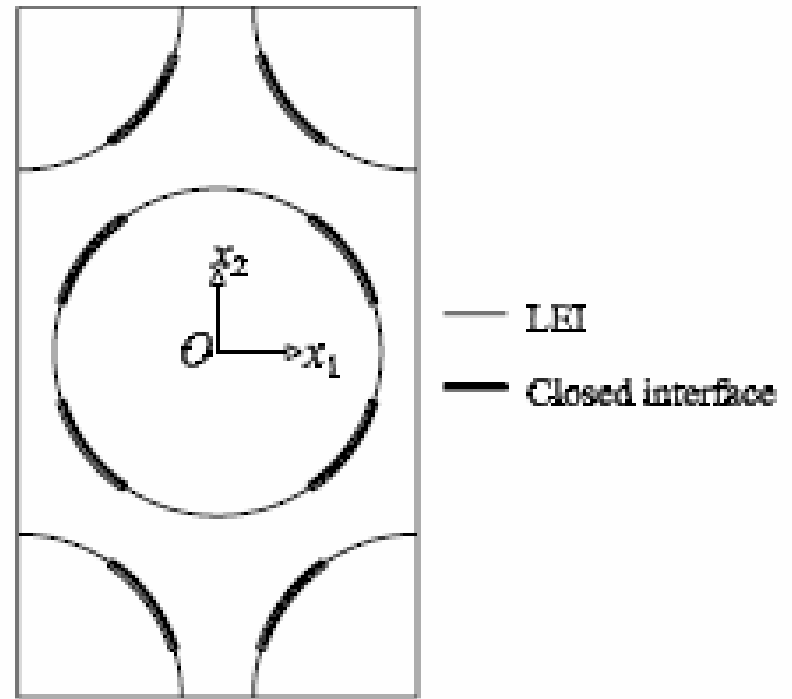
Fig. 8. Case 4.

Deformed mesh:
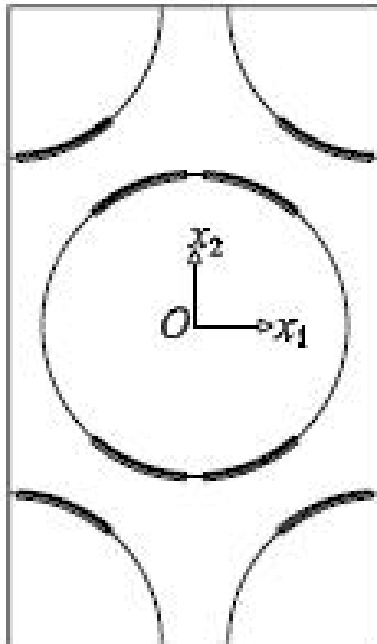
Fig. 9. Case 6.
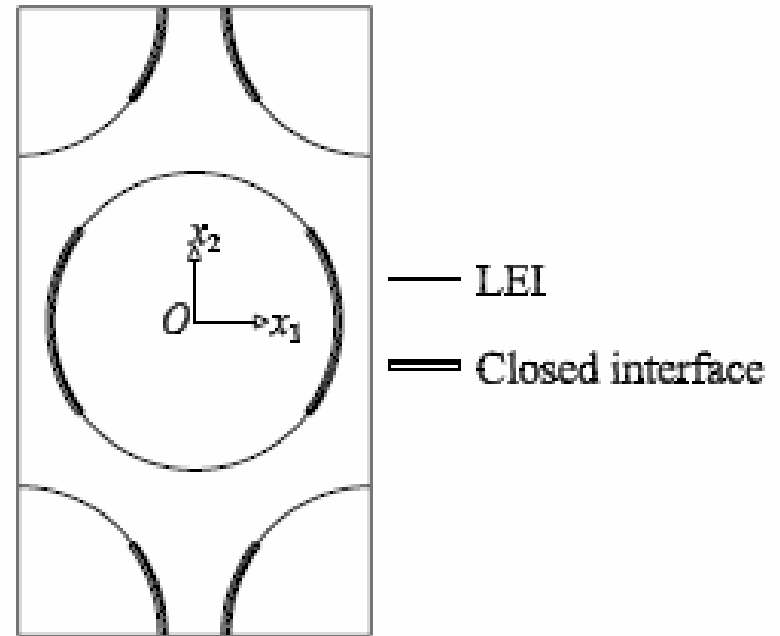
Fig. 10. Case 7.

THANKS FOR YOUR ATTENTION !